European Journal of Pharmaceutical Sciences 198 (2024) 106780

Contents lists available at ScienceDirect

European Journal of Pharmaceutical Sciences

journal homepage: www.elsevier.com/locate/ejps

Predictive computational models for assessing the impact of co-milling on drug dissolution

Nicolas Pätzmann [a,b], Patrick J. O'Dwyer [a], Josef Beránek [b], Martin Kuentz [c], Brendan T. Griffin [a,*]

[a] School of Pharmacy, University College Cork, Cork, Ireland
[b] Department Preformulation and Biopharmacy, Zentiva, k.s., Prague, Czechia
[c] Institute of Pharma Technology, University of Applied Sciences and Arts Northwestern Switzerland, Muttenz, Switzerland

ARTICLE INFO

Keywords:
Co-milling
Co-grinding
Ball milling
Dissolution rate enhancement
In silico modelling
Partial least squares regression
Multiple linear regression

ABSTRACT

Co-milling is an effective technique for improving dissolution rate limited absorption characteristics of poorly water-soluble drugs. However, there is a scarcity of models available to forecast the magnitude of dissolution rate improvement caused by co-milling. Therefore, this study endeavoured to quantitatively predict the increase in dissolution by co-milling based on drug properties. Using a biorelevant dissolution setup, a series of 29 structurally diverse and crystalline drugs were screened in co-milled and physically blended mixtures with Polyvinylpyrrolidone K25. Co-Milling Dissolution Ratios after 15 min ($COMDR_{15\ min}$) and 60 min ($COMDR_{60\ min}$) drug release were predicted by variable selection in the framework of a partial least squares (PLS) regression. The model forecasts the $COMDR_{15\ min}$ ($R^2 = 0.82$ and $Q^2 = 0.77$) and $COMDR_{60\ min}$ ($R^2 = 0.87$ and $Q^2 = 0.84$) with small differences in root mean square errors of training and test sets by selecting four drug properties. Based on three of these selected variables, applicable multiple linear regression equations were developed with a high predictive power of $R^2 = 0.83$ ($COMDR_{15\ min}$) and $R^2 = 0.84$ ($COMDR_{60\ min}$). The most influential predictor variable was the median drug particle size before milling, followed by the calculated drug $logD_{6.5}$ value, the calculated molecular descriptor Kappa 3 and the apparent solubility of drugs after 24 h dissolution. The study demonstrates the feasibility of forecasting the dissolution rate improvements of poorly water-solube drugs through co-milling. These models can be applied as computational tools to guide formulation in early stage development.

1. Introduction

Formulating drugs with dissolution rate limited absorption in oral solid dosage forms remains a challenge for pharmaceutical development (Grady et al., 2018). The Developability Classification System (DCS) enables the identification of potential candidates with dissolution rate limited absorption in the early stage drug development (Butler and Dressman, 2010). For drug candidates with dissolution rate limited absorption (DCS class IIa drugs) the DCS proposes a target particle size to be achieved, below which the risk of dissolution rate limiting the extent of absorption is considered low. Recently, further advancements have been proposed for calculating the appropriate degree of particle size reduction needed to mitigate dissolution limitations for DCS Class IIa drug candidates (Beran et al., 2023). These approaches are already good starting points for identifying and addressing dissolution rate limitations of emerging drug candidates in the early phase of drug development. In practice, reducing drug particles by milling to a calculated size may not be sufficient in every case to overcome dissolution rate absorption. For these scenarios, the inclusion of excipients as a milling aid may be required to further bioenhance the drug in order to achieve desired drug absorption.

Numerous studies have confirmed that the dissolution rate of drugs can be successfully improved by various formulation strategies such as micronisation, spray drying, solid dispersions, inclusion complexes and co-milling (Ibraheem and Wagner, 2021; Saharan et al., 2010). Co-milling has been identified as an industrially scalable, solvent-free and green process in which a drug powder is milled with an excipient to improve its dissolution rate (Maggi et al., 2013; Varghese and Ghoroi, 2017). The process not only promotes mixing and reduces particle size, but can also induce drug amorphization. Additionally, specific

* Corresponding author at: University College Cork, Ireland.
E-mail address: Brendan.Griffin@ucc.ie (B.T. Griffin).

https://doi.org/10.1016/j.ejps.2024.106780
Received 10 February 2024; Received in revised form 12 April 2024; Accepted 27 April 2024
Available online 30 April 2024

drug-excipient interactions and other mechanisms may come into play (Slámová et al., 2021). Therefore, it is assumed that a combination of different factors is responsible for the improvement of the dissolution rate (Brokešová et al., 2022; Vogt et al., 2008).

Polyvinylpyrrolidone (PVP) has been demonstrated in various studies to be a promising excipient for co-milled formulations (Patterson et al., 2007; Chingunpitak et al., 2008; Patterson et al., 2007; Yang et al., 2012). The polymer exhibits the potential to stabilize the produced amorphous state of co-milled drugs leading to an enhanced dissolution rate of the drug (Asgreen et al., 2020; Meiland et al., 2022). Prior investigations with PVP as an excipient in co-milled formulations confirmed successful dissolution rate enhancement of a few drug candidates (Bolourchian et al., 2019; Mura et al., 2002). However, data-driven, computational approaches based on a high-throughput screening to predict drug dissolution after co-milling are lacking.

To guide industrial scientists in the development of orally administered formulations, data-driven prediction models were established in recent years (Bannigan et al., 2021). Considerable progress has been made in computational models for solubility prediction, covering a wide range of models, such as quantitative structure property relationships (QSPR) (Kuentz and Bergström, 2021). By utilising obtained predictive models, industrial scientists can move beyond the traditional trial-and-error approach and adopt more rational procedures that anticipate outcomes. For example, QSPR models for lipid-based formulations to assess the solubility gain helped to streamline the industrial development of drugs with solubility limited absorption by unlocking early indicators of success (Alskär and Bergström, 2015; Bennett-Lenane et al., 2021; Bergström et al., 2016). However, for the development of oral solid dosage forms containing drugs with dissolution rate limited absorption, such QSPR models for a technique to improve dissolution rate have not yet been developed.

The objective of this study was therefore to explore the establishment of a computational model that could be applied for early stage industrial development to predict dissolution rate enhancement achieved by co-milling based on drug properties. The experimental aims were to screen 29 drugs in binary co-milled mixtures (COM) and blended physical mixtures (PM) with PVP. Obtained dissolution profiles combined with measured and calculated drug properties were used for computational modelling.

2. Materials and methods

2.1. Materials

Sertraline, ceritinib, etoricoxib, rivaroxaban, enzalutamide, candesartan cilexetil and PVP K25 were provided by Zentiva, k.s. (Prague, Czechia), apremilast, ezetimibe, tadalafil and dasatinib by MSN Pharmaceuticals Inc. (New Jersey, USA), apixaban and aripiprazole by Sanofi S.A. (Paris, France), nilotinib by Teva Pharmaceutical Industries Limited (Petach Tikwa, Israel), celecoxib by Cadila Pharmaceuticals (Ahmedabad, Gujarat, India), deferasirox by Neuland Laboratories Ltd. (Telangana, India), olaparib by Taizhou Crene Biotechnology Co. Ltd. (Taizhou Zhejiang, China) and sorafenib by Qilu Antibiotics Pharmaceutical Co., Ltd. (Jinan, China). Further model drugs cinnarizine, glibenclamide, griseofulvin, dipyridamole, fenofibrate, albendazole, mefenamicacid, gemfibrozil, carbamazepine, indomethacin, thiabendazole and nimesulide were purchased from Sigma-Aldrich (Prague, Czechia). Reagents for the medium sodium chloride, sodium hydroxide, di-sodium hydrogen phosphate were provided by Sigma-Aldrich (Prague, Czechia) and Simulated Intestinal Fluids powder was sourced from Biorelevant.com Ltd. (London, United Kingdom).

2.2. Compound selection and characteristics

29 poorly water-soluble model drugs with diverse molecular structures and physicochemical properties were selected (Table 1). The dataset contains substances with a wide range of molecular weight (201.3–610.7 g/mol), lipophilicity (calculated $logD_{6.5}$ 1.2–5.2),

Table 1
Selection of physicochemical and molecular properties of investigated compounds.

Drug compound	Molecular weight [g/mol]	Calculated $logD_{6.5}$	Acidic/Basic/Neutral/Ampholyte	Calculated PSA [Å^2]	HBA	HBD	RBC
Albendazole	265.34	2.81	Ampholyte	67.01	4	2	6
Apixaban	459.51	2.16	Neutral	110.76	8	1	3
Apremilast	460.51	1.81	Neutral	119.08	9	1	9
Aripiprazole	448.39	4.08	Basic	44.81	5	1	7
Candesartan Cilexetil	610.67	2.89	Ampholyte	143.34	10	1	10
Carbamazepine	236.28	2.40	Basic	46.33	3	1	1
Celecoxib	381.38	3.81	Acidic	77.98	4	1	2
Ceritinib	558.15	2.60	Ampholyte	105.24	8	3	9
Cinnarizine	368.53	4.08	Basic	6.48	2	0	5
Dasatinib	488.01	2.30	Basic	106.51	9	3	7
Deferasirox	373.37	1.16	Acidic	108.47	6	3	0
Dipyridamole	504.64	2.96	Basic	145.44	12	4	12
Enzalutamide	464.44	3.57	Neutral	76.44	6	1	4
Etoricoxib	358.85	3.35	Basic	59.92	4	0	1
Ezetimibe	409.44	4.18	Neutral	60.77	4	2	6
Fenofibrate	360.84	5.20	Neutral	52.60	4	0	5
Gemfibrozil	250.34	2.41	Acidic	46.53	3	1	6
Glibenclamide	494.01	3.84	Acidic	113.6	8	3	10
Griseofulvin	352.77	2.51	Neutral	71.06	6	0	3
Indomethacin	357.79	1.45	Acidic	68.53	4	1	3
Mefenamic acid	241.29	2.36	Acidic	49.33	3	2	2
Nilotinib	529.53	4.97	Basic	97.62	7	2	5
Nimesulide	308.31	2.45	Acidic	101.22	6	1	4
Olaparib	434.47	2.26	Neutral	86.37	6	1	5
Rivaroxaban	435.89	1.97	Neutral	88.18	8	1	5
Sertraline	306.24	2.56	Basic	12.03	1	1	2
Sorafenib	464.83	5.00	Basic	92.35	7	3	8
Tadalafil	389.41	1.60	Neutral	74.87	6	1	1
Thiabendazole	201.25	2.31	Basic	41.57	2	1	0

The $logD_{6.5}$ and polar surface area values were calculated using ADMET Predictor software (Version 9.5, Simulation Plus, California, USA). Following abbreviations were used: Calculated decadic logarithm of the distribution coefficient (Octanol/water) at pH 6.5 ($clogD_{6.5}$); polar surface area (PSA); number of hydrogen bond acceptors (HBA); number of hydrogen bond donors (HBD); rotatable bond count (RBD).

hydrogen bond acceptors (1–12), hydrogen bond donors (0–4) and rotatable bonds (0–12). Acidic, basic, neutral and ampholyte compounds were included to enhance the structural diversity of the dataset. All model drugs have UV-light absorbing chromophores to enable quantitative determination during dissolution test using an in-situ UV probe.

2.3. Preparation of COM, PM and milled drugs

COM and milled drugs were prepared using a vibrational ball mill (MM 200, Retsch, Haan, Germany). A drug to excipient ratio of 1:2 (w/w) was chosen for the preparation of COM. 250 mg (± 0.1 mg) of a model drug, 500 mg (± 0.2 mg) of PVP K25 and three 9 mm stainless steel balls were placed in a 25 mL stainless steel milling jar. The milling process took 15 min at a frequency of 15 Hz. To prepare the milled drug samples (i.e., milled drug without PVP K25 present), the same preparation process was carried out without the addition of an excipient.

PM of a model drug and PVP K25 in a ratio of 1:2 (w/w) were mixed in a 3D shaker mixer (Turbula type T2F, WAB AG, Switzerland). A 250 mL glass container was filled with 250 mg (± 0.1 mg) of model drug and 500 mg (± 0.2 mg) of PVP K25. The mixing conditions were set to 10 min and 50 rpm.

2.4. Dissolution medium preparation

Fasted State Simulated Intestinal Fluid (FaSSIF) has been produced in accordance with the standard operating procedures provided by biorelevant.com Ltd. The pH was adjusted to 6.50 (± 0.05) and the medium was used within 24 h.

2.5. Dissolution tests and apparent solubility measurements

Dissolution was tested in a USP2 vessel with a stirring speed of 50 rpm in 250 mL FaSSIF at 37 °C. Using fibre-optic UV probes connected to the Rainbow Dynamic Dissolution Monitor Instrument (Pion Inc., Billerica, MA, USA), the duration of the dissolution experiments were 80 min. Standard curves were established using the second derivative of the UV absorbance. The highest wavelength and a range of 10 nm were chosen to generate seven-point calibration curves with an R^2 of > 0.99 for each compound. Depending on the UV absorbance of the drug, a UV probe with a path length of 2, 5 or 10 mm was used. The freshly prepared samples (120 ± 30 min after preparation) were added to the medium in triplicate.

The dose added to dissolution tests corresponded to three times the apparent solubility after 24 h of dissolution which was measured in the same instrument at a stirring speed of 100 rpm in 250 mL FaSSIF V1, 37 °C ($n = 3$) with the pure drug. An excess amount of the drug compound was added to the medium and the average concentration after 24 h calculated to obtain the apparent solubility.

2.6. Particle size distribution

The particle size distribution was measured for 29 poorly water-soluble drugs by laser diffraction analysis (Mastersizer 2000 with Hydro 2000S, Malvern Instruments Co. Ltd., Solihull, UK). Drug powders (200 mg) were added to 50 mL of water and 0.05 mL of Tween 80. To prepare a dispersion, the samples were stirred and mixed for 10 min (± 30 s) and then immediately placed in the Hydro S instrument until a stable obscuration between 10 and 20% was achieved. The refractive index for the dispersion medium water was set to 1.33 and for the particles the values were selected according to refractive indices of the respective compounds from published data. The stirring speed was set to 2100 rpm and the measurement took 30 s. All measurements were carried out in triplicate and average values calculated. Since the highest measured apparent FaSSIF solubility of the drugs in the study was 667 μg/mL (supplementary materials, Table S1) and the prepared dispersions contained a concentration of 4000 μg/mL in water, it can be assumed that highly saturated dispersions were prepared.

2.7. X-Ray powder diffraction (XRPD)

X-ray powder diffraction analyses were performed to evaluate changes in the solid state after milling of powders and mixtures. Powder X-ray diffractograms were collected using a Bruker-AXS D8 Advance powder diffractometer (Karlsruhe, Germany). A CuKα radiation (λ = 1.5418 Å) operated at 40 kV, 40 mA and ambient temperature. The theta-theta geometry ranges from 2 to 40° with a scan rate of 0.02°/s. The generated diffractograms were treated with standard background subtraction and smoothing procedures and the crystallinity of PM and COM was determined by automatized refinement procedures. XRPD patterns were aligned with published data of investigated compounds to confirm their identity.

2.8. Calculation of Co-Milling Dissolution Ratios

The measured released drug concentration [μg/mL] after timepoint n [min] of dissolution of COM $c(\text{drug}_{\text{n min, COM}})$ and PM $c(\text{drug}_{\text{n min, PM}})$ were used to calculate the Co-Milling Dissolution Ratio (COMDR) for 29 drugs at different timepoints via Eq. (1)

$$\text{COMDR}_{\text{n min}} = \frac{\bar{x}\ \text{COM}_{\text{n min}}}{\bar{x}\ \text{PM}_{\text{n min}}} \tag{1}$$

where $\bar{x}\ \text{COM}_{\text{n min}}$ and $\bar{x}\ \text{PM}_{\text{n min}}$ describe the mean concentration of released drug after n min dissolution of a COM and of a PM.

The standard error of COMDR was calculated from Eq. (2) (Fagerberg et al., 2012):

$$\text{SE}_{\text{COMDR}} = \text{COMDR} * \sqrt{\frac{\text{SE}_{\bar{x}\text{COM}}{}^2}{\bar{x}\text{COM}^2} + \frac{\text{SE}_{\bar{x}\text{PM}}{}^2}{\bar{x}\text{PM}^2}} \tag{2}$$

$\text{SE}_{\bar{x}\text{COM}}$ and $\text{SE}_{\bar{x}\text{PM}}$ are the standard errors of the mean concentration of released drug in the respective mixtures.

2.9. Statistics and model development

To investigate the influence of molecular, physicochemical and measured drug properties on the improvement of dissolution after co-milling with PVP K25, multivariate data analysis was performed using Simca (Version 15.0, Sartorius, Germany). ADMET Predictor software (Version 9.5, Simulation Plus, USA) was used to generate molecular descriptors. SMILES strings of all model drugs were obtained from PubChem as inputs for the ADMET Predictor and compounds were randomly assigned to training and test sets. A principal component analysis (PCA) and a Hotelling T2 ellipse (95% confidence interval) of all descriptors were performed to identify potential outliers that would have been assigned to the test set to avoid such compounds affecting the training set. Partial least squares projection to latent structures (PLS) models were developed to identify important variables and for quantitative predictions. Descriptors from ADMET Predictor, results of particle size distribution measurements (D50) and the measured apparent solubility in FaSSIF after 24 h dissolution values were added to the dataset and used as inputs for PLS modelling. The logarithm of the COMDR after 15 and 60 min of dissolution were used as response. In a first step, the descriptors were de-identified and standardised by mean centering and scaled to unit variance. Calculated descriptors with the same value for all model drugs were removed. Subsequently, 244 standardised descriptors were submitted for variable selection. Based on the Variables of Importance in Projection (VIP) diagram, all variables except the 100 most important for the response were excluded. In a next step, variables whose exclusion resulted in an increase or no change in R^2 and Q^2 were permanently removed from the model. Q^2 was validated using 7 leave-one-out cross-validation groups. To ensure accuracy, PLS regressions

were validated using root mean square error of cross validation ($RMSE_{CV}$) and permutation tests (100 iterations). Final models were validated with the test sets. A limit of four variables resulting in a maximum Q^2 value were selected to avoid overfitting.

Multiple linear regression (MLR) equations to quantitatively predict Co-Milling Dissolution Ratios were generated using SPSS Statistics (Version 26, IBM Corporation, US). MLR equations were established based on selected variables from PLS models. The combination of three of the four variables selected in PLS models that yielded the highest R^2 values was used to generate MLR equations, considering multicollinearity. The same training and test sets were employed as for the PLS models.

3. Results and discussion

3.1. Dissolution profiles

Fig. 1 illustrates the dissolution profiles of 29 structurally diverse

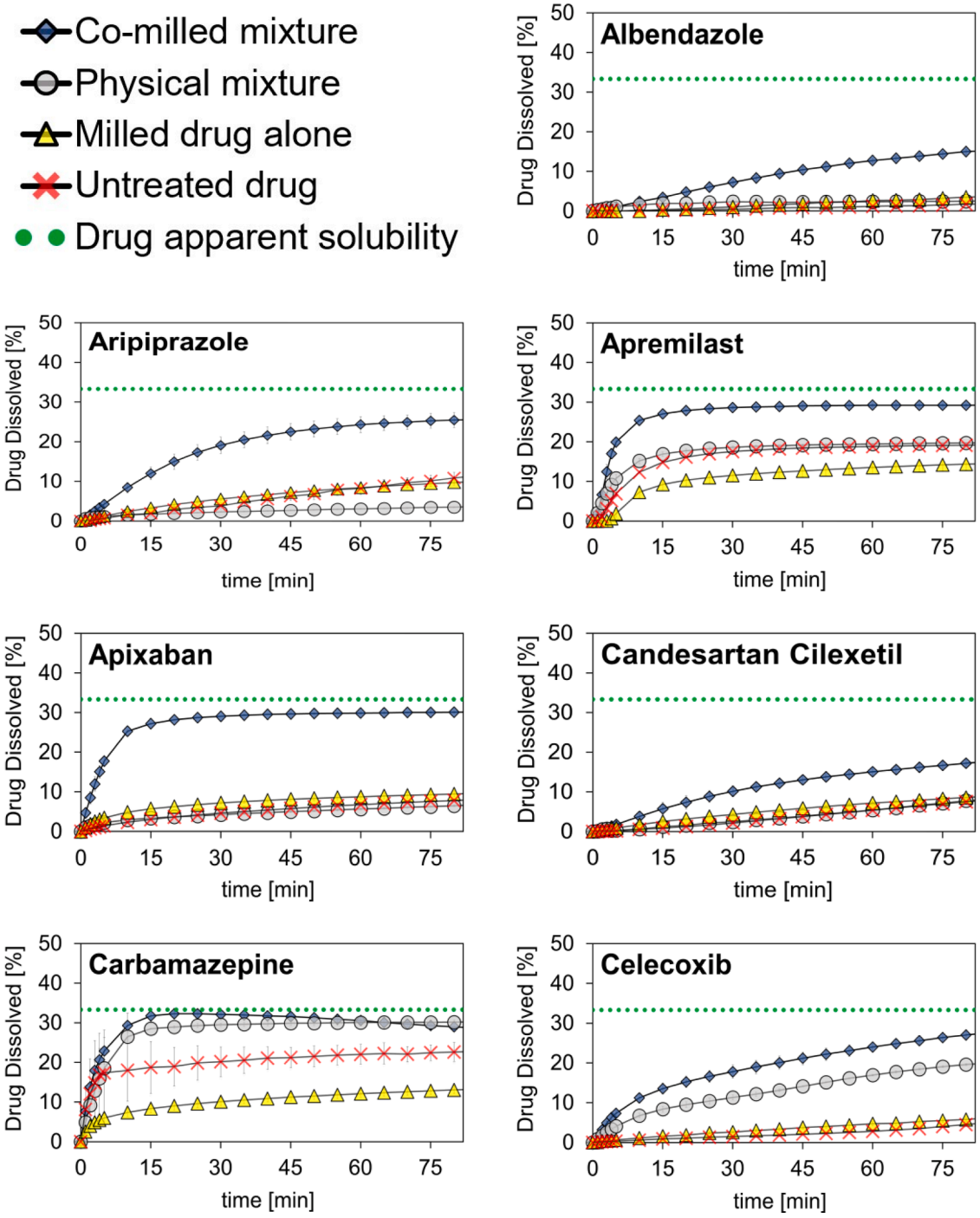

Fig. 1. Dissolution profiles of untreated drug powders, milled drug powders, binary physical and co-milled mixtures with PVP K25 as carrier for 29 compounds are shown. Depicted as blue squares are measurement points of co-milled mixtures, those of physical mixtures are grey filled circles, the unmilled drug powders are shown as red crosses and the dissolution profiles of milled drug powders are labelled as yellow triangles. The apparent solubility after 24 h dissolution of each drug is plotted as a green dotted line. An excess of three times the apparent solubility of each drug was added to the dissolution experiments. Some error bars are small and only barely visible.

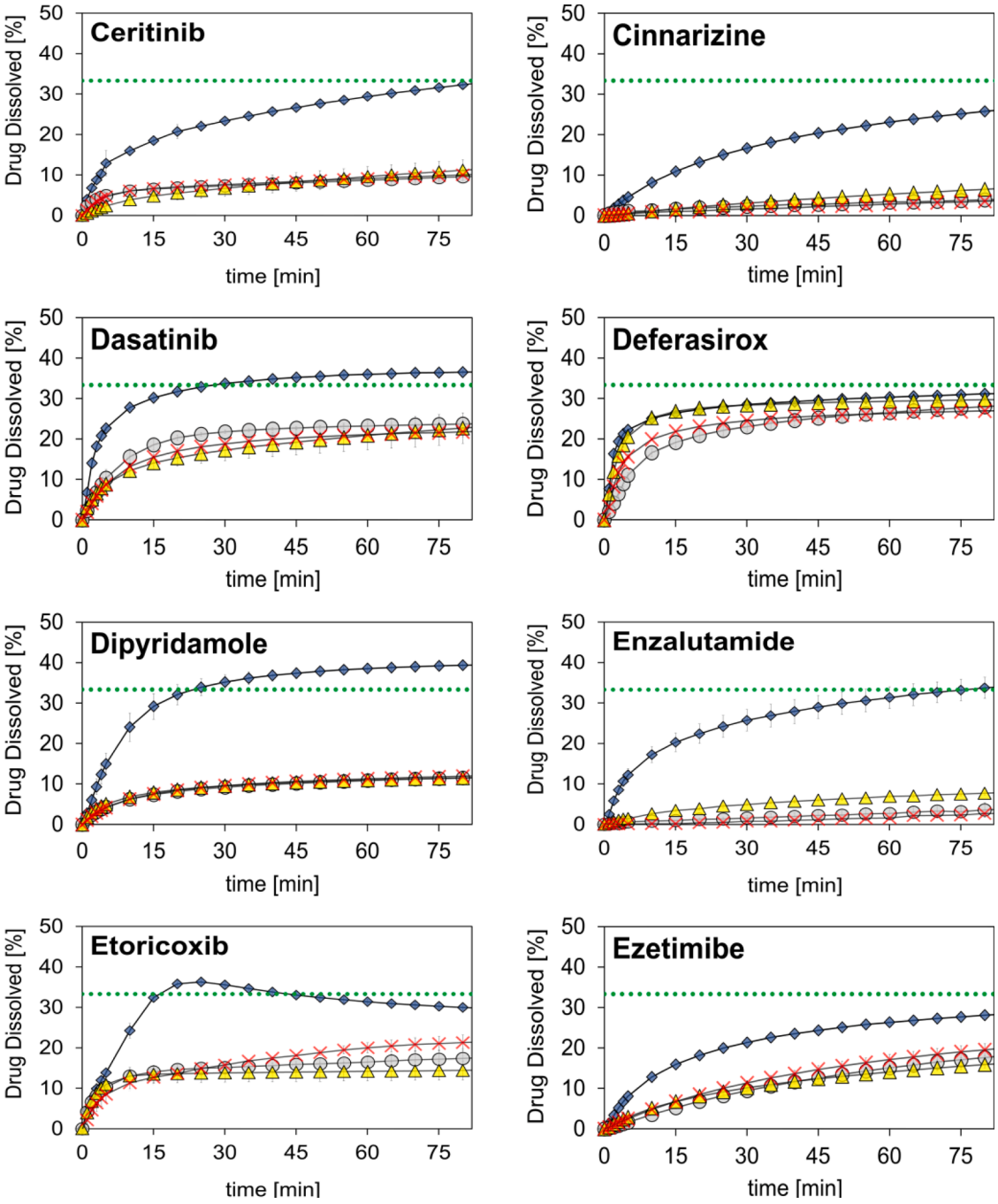

Fig. 1. (*continued*).

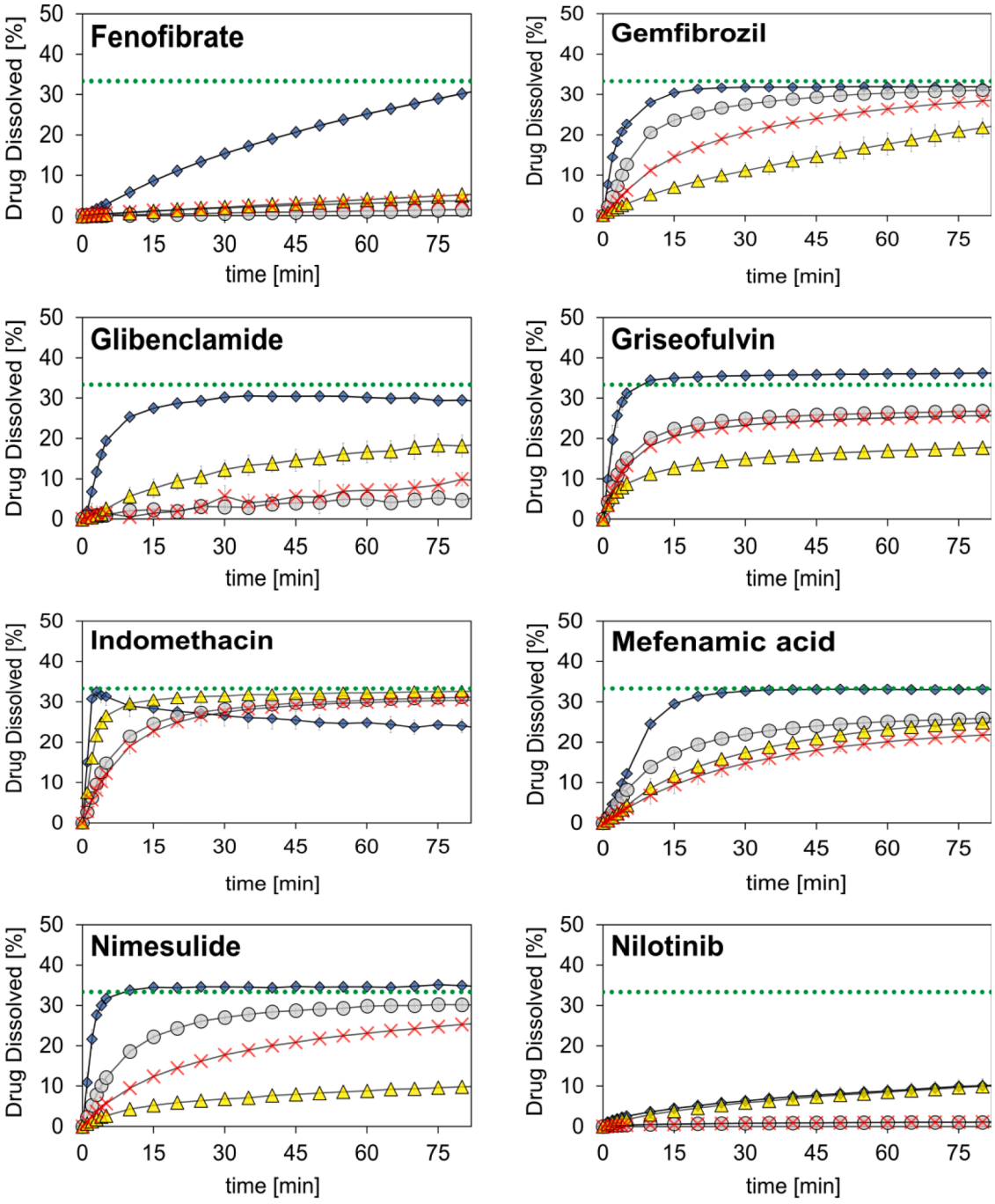

Fig. 1. (*continued*).

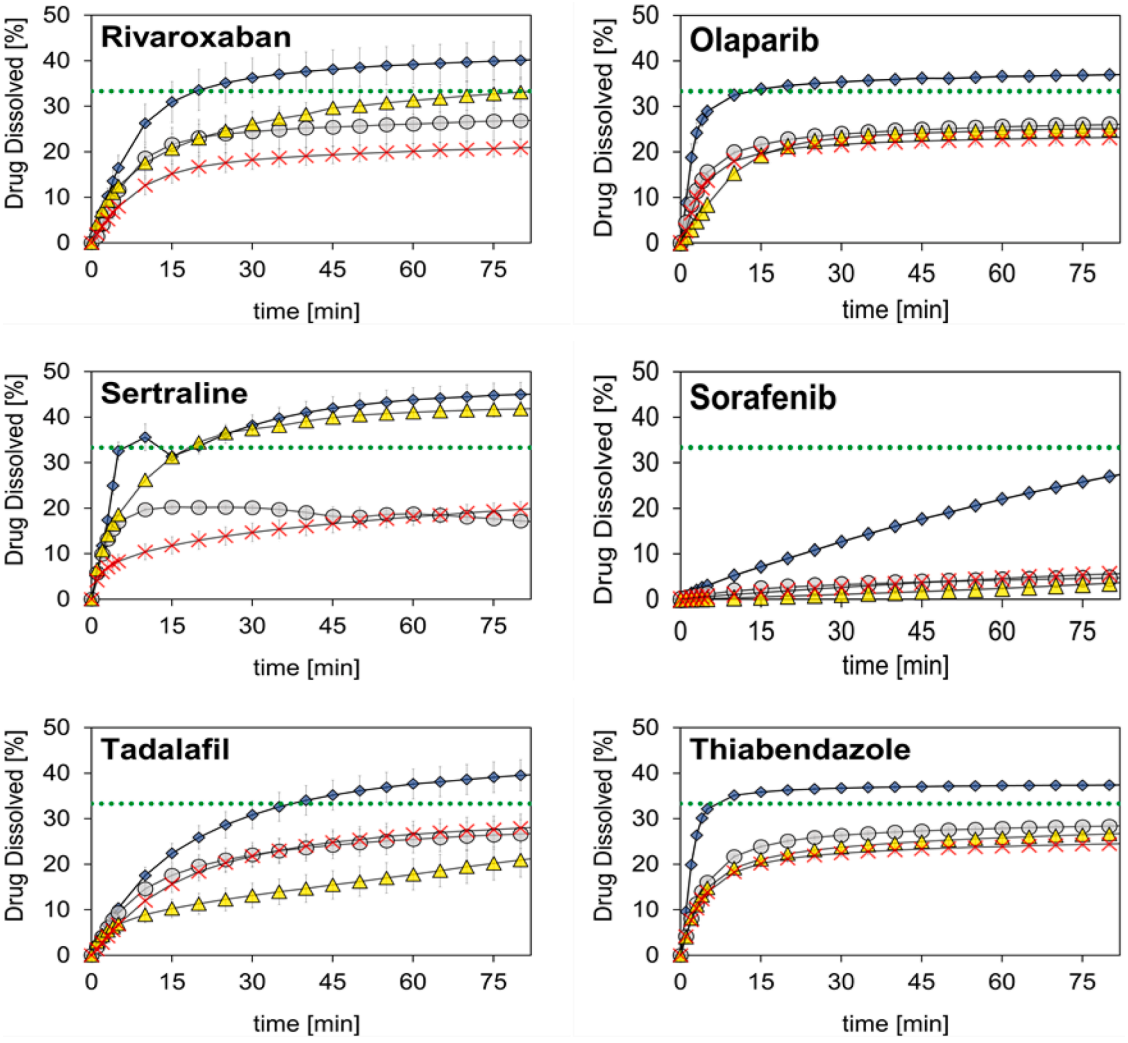

Fig. 1. (*continued*).

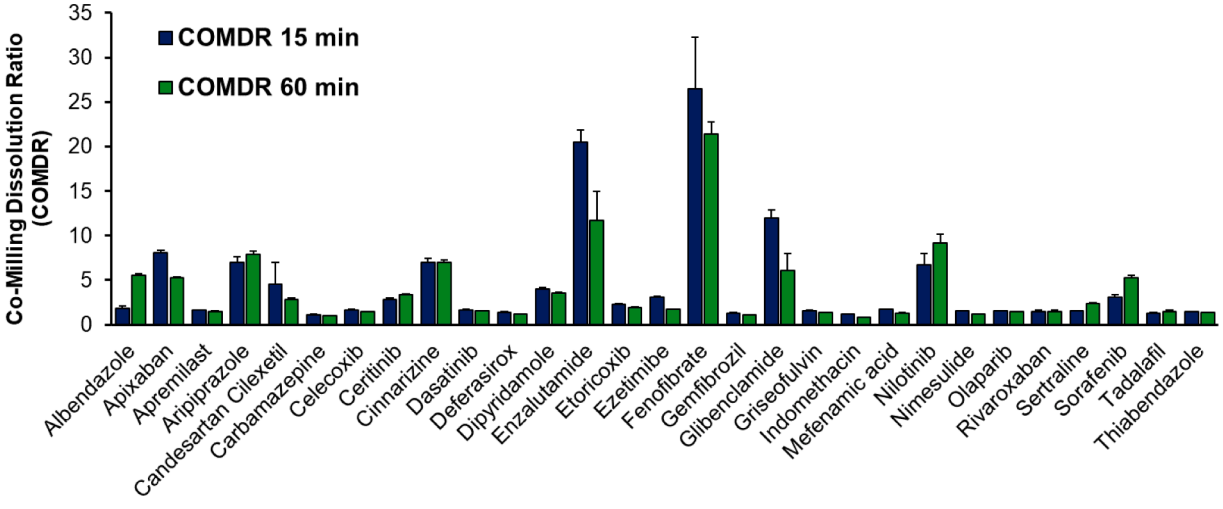

Fig. 2. Co-Milling Dissolution Ratios (COMDR) of all 29 drugs used in the study with standard errors after 15 min (green) and 60 min (blue) of dissolution ($n = 3$). The COMDR is the ratio of mean released drug concentration in co-milled and physical mixtures with PVP K25 in a drug to excipient ratio of 1 to 2 (w/w) at above mentioned timepoints.

drug substances under different processing conditions, i.e. as unmilled powder, milled powder, PM and COM. For the evaluation of dissolution profiles, one timepoint in the early phase (15 min) of the dissolution process and one timepoint in a later stage (60 min) of COM and PM were selected. The 15 min and 60 min dissolution timepoints are of industrial relevance to achieve specifications in bioequivalence studies to prove similarity of dissolution profiles and biowaiver approvals of immediate release formulations (Ono et al., 2023).

Considering the 15 min timepoint, the $COMDR_{15\ min}$ ranges from 1.11 (carbamazepine) to 26.48 (fenofibrate) (Fig. 2 and supplementary materials, Table S3). In 26 of 29 cases, a two-sided *t*-test showed a significantly higher dissolved drug concentration from COM compared to PM ($p < 0.05$). Non-significant differences were observed for tadalafil ($p = 0.055$), rivaroxaban ($p = 0.051$) and indomethacin ($p = 0.064$). These compounds have in common that the measured unmilled median drug particle sizes were amongst the smallest in the dataset (tadalafil = 15.89 ± 3.89 µm; rivaroxaban = 9.5 ± 1.54 µm; carbamazepine = 15.87 ± 2.74 µm). Further, the calculated $logD_{6.5}$ values of these compounds were low which suggests that these compounds are amongst the least lipophilic within the dataset (tadalafil 1.60; rivaroxaban 1.97; carbamazepine 2.40). It may reflect that these compounds benefit less from the potential wetting enhancement and subsequent dissolution enhancement through their embedding in the polymer matrix than more lipophilic compounds.

After 60 min of dissolution, fenofibrate was the drug substance with the highest COMDR with a value of 21.48 and indomethacin the lowest with 0.82 (Fig. 2 and supplementary materials, Table S4). Fenofibrate has the largest particle size (255.3 ± 3.4 µm) and the calculated lipophilicity, expressed by clogD6.5 (5.2), of the investigated drugs. In the entire screening, indomethacin is the only substance with a lower dissolved concentration in COM than in PM after 60 min ($p = 0.005$). No significant differences could be measured for carbamazepine ($p = 0.46$). Within the 27 remaining compounds, a higher concentration of the drug was released from COM than from PM after 60 min of dissolution ($p < 0.05$).

The dissolution profiles of co-milled and milled drugs allow to assess the influence of the addition of an excipient to the ball milling process. For 24 out of 29 compounds, the dissolved fraction of the drug was significantly higher from co-milled blends. Dissolution of milled and co-milled sertraline ($p = 0.83$), nilotinib ($p = 0.47$), indomethacin ($p = 0.24$) and deferasirox ($p = 0.068$) did not result in statistically significant differences after 15 min drug release. After 60 min, again sertraline ($p = 0.19$) and nilotinib ($p = 0.77$) did not dissolve to a significantly different degree as well as rivaroxaban ($p = 0.057$). Deferasirox and rivaroxaban revealed very small initial particle sizes (5.2 ± 0.2 and 9.5 ± 1.6 µm) and also low calculated logD6.5 values (deferasirox 1.16 and rivaroxaban 1.97) which may be reasons that the addition of the excipient in a co-milling process did not significantly influence the dissolution enhancement compared to milling the drug without excipient.

The shape of the dissolution profile of co-milled Indomethacin was atypical and did not match standard zero or first order release kinetics. A rapid initial increase in apparent drug concentration was observed during the first two minutes of dissolution. After that initial "spring effect", the measured apparent concentration of indomethacin in FaSSIF decreased slowly, potentially due to partial precipitation in the metastable zone of a dissolution profile with "spring and parachute" characteristics. The spring effect may have been caused by structural disorder and amorphization on drug particle surfaces created during the co-milling process. Recent studies presented the tendency of Indomethacin to transition into the amorphous state by milling with excipients (Iemtsev et al., 2022; Lim et al., 2016)

3.2. Influence of co-milling on solid state properties of drug substances

XRPD measurements were used to investigate whether the milling processes caused polymorphic changes in investigated drugs and to evaluate the loss of crystallinity during co-milling. XRPD patterns are presented in the supplementary materials, Figures S1 – S58. Sharp Bragg peaks in the diffractograms of all model drugs confirmed a high initial degree of crystallinity before milling. In addition, sharp peaks were still visible in all diffractograms of COM after 15 min of drug ball milling with PVP. In 21 of 29 diffractograms of COM, peak intensity was reduced compared to PM, indicating a partial loss of crystallinity due to milling-induced disorder of the solid drug substance particles.

All polymorphs of investigated compounds are listed in supplementary materials, Table S6. The diffractograms of binary mixtures did not result in changes of the basic patterns which suggests that no major polymorphic changes were produced during co-milling of binary mixtures. An exception is an initial polymorphic transformation of ceritinib (polymorphic form 2b) that can be assumed since new peaks are visible in the X-Ray diffractogram of the co-milled mixture. Interestingly, milling of drugs without the addition of the excipient resulted in a polymorphic change of enzalutamide from form R1 to R2. A beginning polymorphic transition of tadalafil was observed which was originally in form a.

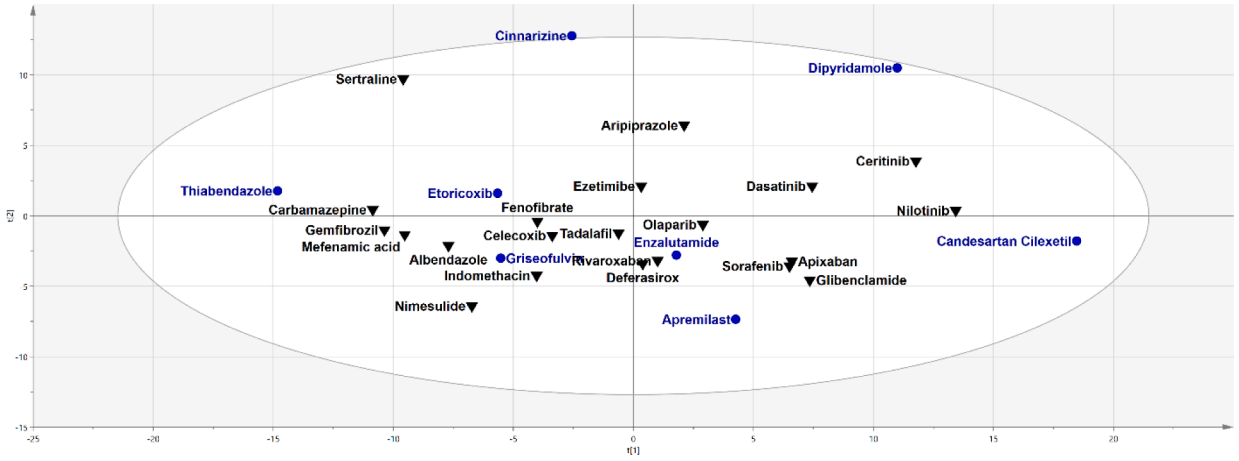

Fig. 3. Principal component analysis of the chemical space based on the calculated molecular properties of investigated compounds. For the development of predictive models, the compounds were randomly assigned to a training set (black) and a test set (blue). Drugs of training and test are well distributed over the chemical space.

Table 2
Results from PLS model development for the logarithm of the ratio of released drug in co-milled and physical mixtures (LogCOMDR) after 15 and 60 min of dissolution.

	R^2	Q^2	$RMSE_{Tr}$	$RMSE_{Te}$	$RMSE_{CV,\ Tr}$	$RMSE_{CV,Te}$	Selected variables
$LogCOMDR_{15\ min}$	0.82	0.77	0.12 ($n = 21$)	0.17 ($n = 8$)	0.15 ($n = 21$)	0.18 ($n = 8$)	D50, $clogD_{6.5}$, Kappa 3, apparent solubility,
$LogCOMDR_{60\ min}$	0.87	0.84	0.13 ($n = 21$)	0.11 ($n = 8$)	0.13 ($n = 21$)	0.12 ($n = 8$)	D50, $clogD_{6.5}$, T_RDmtr, apparent solubility

The following abbreviations are used: Root mean square error (RMSE), Training set (Tr), Test set (Te), Cross Validation (CV), measured median drug particle size (D50), calculated decadic logarithm of the distribution coefficient (Octanol/water) at pH 6.5 ($clogD_{6.5}$), degree of branching at the centre of a molecule (Kappa 3), relative topological diameter of the hydrogen-suppressed molecular graph (T_RDmtr).

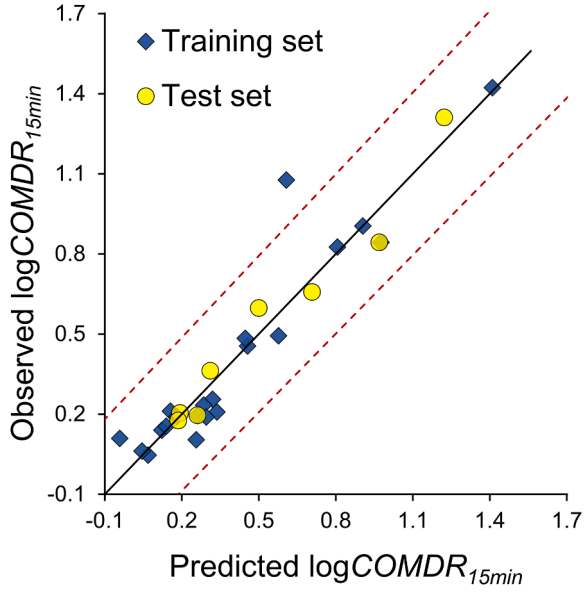

Fig. 4. PLS model results of the logarithm of Co-milling Dissolution Ratios after 15 min of dissolution ($logCOMDR_{15min}$). Drugs in the training set are depicted as blue squares and candidates of the test set as yellow circles.

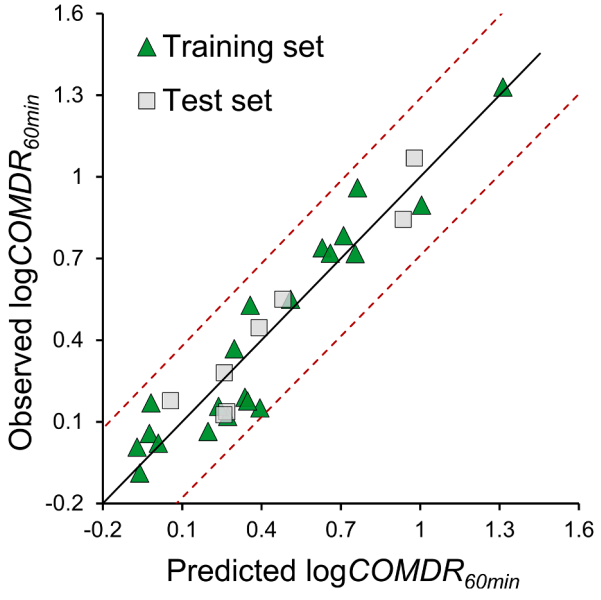

Fig. 5. PLS model results of the logarithm of Co-Milling Dissolution Ratios after 60 min of dissolution ($logCOMDR_{60min}$). Drugs from the training set are shown as green triangles and candidates from the test set are shown as grey squares.

3.3. Prediction of Co-Milling Dissolution Ratios

A PCA based on molecular properties was conducted to initially explore the structural diversity of screened model drugs. The plot confirmed that investigated compounds are covering a wide chemical space as drug substances are well distributed on the PCA-X graph (Fig. 3). Drugs from the training and test set are also widely distributed over the chemical space. Subsequently, PLS models were developed to explore the feasibility of predicting the $COMDR_{15\ min}$ and $COMDR_{60\ min}$. In the framework of PLS modelling, it was examined which properties of drug substances have an influence on the rate of dissolution after applying the co-milling technique with PVP K25. The Variables of Importance in Projection plots of $COMDR_{15\ min}$ and $COMDR_{60\ min}$ are added to supplementary materials, Figure S59 and S60. The logarithm of COMDR at the respective timepoints were used to build linear models. In addition to the calculated molecular properties, measured median particle sizes of drug powders with a broad span of 3.6 μm to 255 μm and apparent solubilities of pure drug substances after 24 h of dissolution were included as variables in the PLS models (Supplementary materials, Tables S1 and S2).

The highest Q^2 value of the training set with $COMDR_{15\ min}$ was obtained with the inclusion of the median particle size (D50) of unmilled drug, the measured apparent solubility of the drug and the calculated molecular descriptors $clogD_{6.5}$ and Kappa 3 (Table 2). An R^2 value of 0.82, a Q^2 value of 0.77 and only small differences in root mean square error ($RMSE_{Tr} = 0.12$, $RMSE_{Te}$ 0.17) and root mean square error of cross validations ($RMSE_{CV,\ Tr} = 0.15$, $RMSE_{CV,\ Te} = 0.18$) of training and test set allow the prediction to be considered as valid. As illustrated in Fig. 4, each value of the test is within the prediction interval of the training set. There is one outlier in the training set (glibenclamide), all other drugs are within the prediction interval of the trained model. The observed $logCOMDR_{15min}$ (1.08) is considerably higher than the predicted $logCOMDR_{15min}$ (0.76). This under-prediction could be a result of the low apparent solubility value of glibenclamide (4.0 ± 0.5 μg/mL), which may not be captured by this model. Since the validation with the test set showed that all substances are in the prediction interval and therefore the outlier appears to not strongly influence the predictive accuracy of the model, the outlier remained in the model.

Another PLS model was developed for the ratio of the 60 min timepoints to detect effects and influences of variables on the further progression of the dissolution process. The variable selection considered again the median particle size D50 and apparent solubility of the pure drug as well as the calculated descriptor $clogD_{6.5}$. This time, the molecular descriptor T_RDmtr ended up in the model instead of Kappa 3 (Table 2). The model achieved a high predictivity ($R^2 = 0.87$, $Q^2 = 0.84$). The root mean square error ($RMSE_{Tr} = 0.13$, $RMSE_{Te} = 0.11$) and the root mean square error of cross validation ($RMSE_{CV,\ Tr} = 0.13$, $RMSE_{CV,\ Te} = 0.12$) of training and test set differ only slightly, confirming a good prediction. All timepoints are in the prediction interval, which is shown graphically in Fig. 5.

The inclusion of a particle size parameter in the models is explainable as reducing the particle size leads to an increase in the drug particle surface area, which according to the Nernst-Brunner equation results in an improvement of dissolution rate (Brunner, 1904; Nernst, 1904).

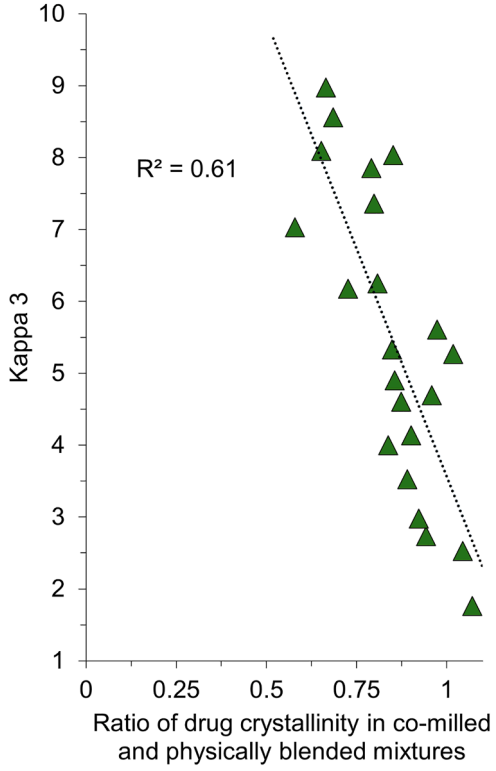

Fig. 6. Correlation between the computationally selected molecular descriptor Kappa 3 and the crystallinity ratio of drugs in co-milled and physically mixed formulations.

Table 3
Summarized results of multiple linear regression equations.

	R^2	$RMSE_{Tr}$	$RMSE_{Te}$	F-value	p-value	Variables
$logCOMDR_{15\ min}$	0.83	0.128 (n = 21)	0.190 (n = 8)	46.52	2.2 *10^{-10}	D50, $clogD_{6.5}$, Kappa3
$logCOMDR_{60\ min}$	0.84	0.117 (n = 21)	0.144 (n = 8)	51.65	7.4 * 10^{-11}	D50, $clogD_{6.5}$, c_s

The following abbreviations are used: Root mean square error (RMSE); Training set (Tr); Test set (Te), measured median drug particle size (D50), calculated decadic logarithm of the distribution coefficient (Octanol/water) at pH 6.5 ($clogD_{6.5}$), degree of branching at the centre of a molecule (Kappa 3), measured apparent solubility of drug in FaSSIF at 37 °C after 24 h dissolution of pure drug substance (c_s).

Co-milling is designed to reduce particle size, and the positive correlation between drug particle size before milling and the enhancement of dissolution rate through co-milling suggests that larger drug particles before co-milling may have a higher potential for size reduction, leading to an increased dissolution rate. However, very small drug particles may have the tendency to aggregate during the milling process.

In contrast to molecular descriptors and substance specific properties, particle sizes vary from batch to batch. Milling of drugs commonly leads to a particle size reduction up to a grinding limit where particle agglomeration and particle size breakage are in equilibrium (Knieke et al., 2009). The grinding limit is the result of a balance between material properties and the energy applied to the drug particles during the milling process (Luciani, 2018). Other batches with different particle sizes would also lead to a reduction in particle size near to the grinding limit and therefore also to a dissolution enhancement which appears to also depend on the particle size of the drug batch. The present model was trained for particle sizes from 3.62 ± 0.03 µm to 255.26 ± 3.35 µm, representing the range for which the model is applicable.

The second parameter present in each model is the lipophilicity/distribution coefficient $clogD_{6.5}$ as calculated by the ADMET predictor, which is a parameter for the lipophilicity of a molecule (Kah and Brown, 2008). The higher the $clogD_{6.5}$ of a molecule, and thus its lipophilicity, the lower may be the wettability of particle surfaces. A poor wettability may result in decreased dissolution rates and several studies confirmed that drug powders embedded in a polymer matrix of a co-milled mixture exhibit increased wettability (Gu et al., 2012; Maggi et al., 2013; Varghese and Ghoroi, 2017). Drugs with more lipophilic surfaces may benefit more from the embedding in polymer matrices by co-milling in terms of wettability, and therefore the dissolution rate can also be improved to a higher extent.

The 15 min model includes the calculated molecular descriptor Kappa 3 which indicates the shape of organic molecules neglecting hydrogen by describing atomic radii and the number of topological paths (Kier, 1985). Bigger and more complex molecules tend to have less rigid structures, which facilitates the formation and persistence of amorphous fractions in molecules (Alhalaweh et al., 2014; Mahlin and Bergström, 2013). In line with this, higher Kappa 3 values may indicate an increased tendency to induce mechanically surface disorder and partial amorphization during co-milling. Derived by automated refinement procedures of X-Ray diffractograms, Fig. 6 demonstrates the relationship between computed Kappa 3 values and the residual drug crystallinity in co-milled formulations. Drug compounds with median particle sizes above 100 µm (apixaban, aripiprazole, enzalutamide and fenofibrate) were excluded since the particle size may influence the reliability of the assessment. The relationship (R^2 = 0.61) between the residual crystallinity of drugs in co-milled formulations and the Kappa 3 value of drug substances indicates that with increasing complexity of molecules, the loss of crystallinity due to co-milling increases and consequently the dissolution rate as extracted from the modelling procedure (Eq. (3)).

Another selected molecular descriptor refers to the topology (T_RDmtr, 60 min COMDR) of the molecule (Bloomingdale and Mager, 2019). The calculated molecular descriptors T_RDmtr and $logD_{6.5}$ provide first indications which properties of a molecule could be associated with a successful dissolution rate enhancement by co-milling.

The results of PLS models were used to generate applicable MLR equations that predict the Co-Milling Dissolution Ratios after 15 and 60 min of dissolution by applying co-milling with PVP K25 based on only three of the selected variables that yielded in the highest R^2 value (Eqs. (3) and (4)). Results of MLR equations are summarized in Table 3. A test of multicollinearity is a requirement for the validity of MLR equations. Multicollinearity exists if the variable inflation factor is greater than 5 or less than 0.2. Furthermore, a conditions index of 10–30 indicates multicollinearity, above 30 a strong multicollinearity (Kim, 2019). The variable inflation factors are 1.1 and 1.6, and the condition indices 7.8 and 8.1, indicating that there is no considerable multicollinearity in the generated MLR equations (Supplementary materials, Table S5). These identified equations would be readily applied in early stage drug development to guide formulators on the potential improvements in

Table 4
Beta Standardized coefficients of variables selected for multiple linear regression equations.

	D50	$clogD_{6.5}$	Kappa 3	c_s
$logCOMDR_{15\ min}$	0.284	0.105	0.095	–
$logCOMDR_{60\ min}$	0.214	0.154	–	−0.077

The following abbreviations are used: Median drug particle size (D50), calculated decadic logarithm of the distribution coefficient (Octanol/water) at pH 6.5 ($clogD_{6.5}$), degree of branching at the centre of a molecule (Kappa 3), measured apparent solubility of drug in FaSSIF at 37 °C after 24 h dissolution of pure drug substance (c_s).

dissolution via co-milling.

$$\log COMDR_{15min} = -0.319 + 0.00377 * D50 + 0.098 * clogD_{6.5} + 0.05 * Kappa3 \quad (3)$$

$$\log COMDR_{60min} = -0.141 + 0.00325 * D50 + 0.142 * clogD_{6.5} - 0.00051 * c_s \quad (4)$$

The generated MLR equations have R^2 values of 0.83 and 0.84, indicating a high predictivity (Table 3). Importantly, the difference between RMSE values were small which suggests that valid prediction models were given in line with the obtained *p*-values. In both formulas, the median particle size of the original drug powder and the $clogD_{6.5}$ values were included in the equations. For the 15 min timepoint, the calculated molecule descriptor Kappa 3 was included as a third descriptor, whereas at the 60 min timepoint, the measured apparent solubility was included. The different equations for early and later stage timepoints were data-driven findings, but it can be also justified from a mechanistic viewpoint. The presence of Kappa 3 in the dissolution formula at 15 min, and its absence at 60 min, may refer to produced high-energy sites on the surface of drug particles. Such high energy sites would be expected as surface-induced disorder that can progress from the surface to a more pronounced partial amorphization (Niederquell and Kuentz, 2014). Nevertheless, these effects are anticipated to be less significant in the later stages of dissolution. Therefore, it makes sense to employ separate models for the early and later stages.

To estimate the influence of every variable on the Co-Milling Dissolution Ratios, beta standardized coefficients of MLR equations were calculated. At the time of 15 min, all variables contributed positively to the increase in the amount released in co-milled materials, i.e., the higher the median particle size D50, $clogD_{6.5}$, and Kappa 3 values of the drug substance the greater the expected increase in the proportion of dissolved drug after co-milling (Table 4). The size of the median particle had the biggest influence on the $COMDR_{15\ min}$ (0.284), followed by $clogD_{6.5}$ (0.105) and Kappa 3 (0.095). After 60 min of dissolution the median particle size had again the highest influence on the COMDR (0.214) followed again by $clogD_{6.5}$ (0.154). The apparent solubility contributed with −0.077 negatively to the $COMDR_{60\ min}$ which means that the higher the apparent solubility was, the lower tends to be the expected $COMDR_{60\ min}$.

The purpose of this study was to develop a co-milling model that is specifically designed for dissolution rate limitations in industry. Thus, a comparatively short milling time of 15 min was selected for this study. By applying longer co-milling times the production of structural disorder and amorphous regions is expected to increase which could be of interest to improve the solubility of the compounds (Asgreen et al., 2020). A limitiation of this study is that the whole model was performed only with PVP. As a consequence, outcomes of the study may not be generalisable to other excipients. In addition, the characterization of 29 drugs in the field of pharmaceutics is a large data set, which, however, represents a relatively small dataset from the perspective of theoretical data science. An extended dataset would therefore be desirable to enable a broader applicability of co-milling in pharmaceutical drug development.

4. Conclusion

This study successfully predicted the impact of co-milling with PVP on the dissolution of drug compounds. The key factors were identified as the median particle size of drug powders, the calculated molecular descriptors $clogD_{6.5}$ and Kappa 3, and the apparent solubility of drugs. Multiple linear regression equations were derived based on computationally selected variables, making them suitable for industrial applications. Future studies could further validate established in silico predictions of this work to enable rational decision-making in the development of co-milled formulations.

CRediT authorship contribution statement

Nicolas Pätzmann: Writing – original draft, Visualization, Validation, Software, Methodology, Investigation, Formal analysis, Data curation, Conceptualization. **Patrick J. O'Dwyer:** Writing – review & editing, Supervision, Project administration, Methodology, Investigation, Conceptualization. **Josef Beránek:** Writing – review & editing, Supervision, Resources, Project administration, Methodology, Investigation, Funding acquisition, Conceptualization. **Martin Kuentz:** Writing – review & editing, Supervision, Project administration, Methodology, Investigation, Funding acquisition, Conceptualization. **Brendan T. Griffin:** Writing – review & editing, Supervision, Project administration, Methodology, Funding acquisition, Conceptualization.

Declarations of competing interest

The authors report no declarations of interest.

Data availability

Data will be made available on request.

Acknowledgements

This project has received funding from the European Union`s Horizon 2020 research and innovation programme under the Marie Curie Sklodowska-Curie grant agreement No 955756.

We would like to thank Ondřej Dammer, Michal Šimek and Hana Tožičková for their cooperation in XRPD measurements and Marek Štika for helpful suggestions and discussions on developing dissolution methods.

Supplementary materials

Supplementary material associated with this article can be found, in the online version, at doi:10.1016/j.ejps.2024.106780.

References

Alhalaweh, A., Alzghoul, A., Kaialy, W., Mahlin, D., Bergström, C.A.S., 2014. Computational predictions of glass-forming ability and crystallization tendency of drug molecules. Mol. Pharm. 11, 3123–3132. https://doi.org/10.1021/mp500303a.

Alskär, L.C., Bergström, C.A.S., 2015. Models for predicting drug absorption from oral lipid-based formulations. Curr. Mol. Biol. Rep. 1, 141–147. https://doi.org/10.1007/s40610-015-0023-1.

Asgreen, C., Knopp, M.M., Skytte, J., Löbmann, K., 2020. Influence of the polymer glass transition temperature and molecular weight on drug amorphization kinetics using ball milling. Pharmaceutics 12, 483. https://doi.org/10.3390/pharmaceutics12060483.

Bannigan, P., Aldeghi, M., Bao, Z., Häse, F., Aspuru-Guzik, A., Allen, C., 2021. Machine learning directed drug formulation development. Adv. Drug Deliv. Rev. 175, 113806 https://doi.org/10.1016/j.addr.2021.05.016.

Bennett-Lenane, H., O'Shea, J.P., Murray, J.D., Ilie, A.-R., Holm, R., Kuentz, M., Griffin, B.T., 2021. Artificial neural networks to predict the apparent degree of supersaturation in supersaturated lipid-based formulations: a pilot study. Pharmaceutics 13, 1398. https://doi.org/10.3390/pharmaceutics13091398.

Beran, K., Hermans, E., Holm, R., Sepassi, K., Dressman, J., 2023. Projection of target drug particle size in oral formulations using the refined developability classification system (rDCS). Pharmaceutics 15. https://doi.org/10.3390/pharmaceutics15071909.

Bergström, C.A.S., Charman, W.N., Porter, C.J.H., 2016. Computational prediction of formulation strategies for beyond-rule-of-5 compounds. Adv. Drug Deliv. Rev. 101, 6–21. https://doi.org/10.1016/j.addr.2016.02.005.

Bloomingdale, P., Mager, D.E., 2019. Machine learning models for the prediction of chemotherapy-induced peripheral neuropathy. Pharm. Res. 36, 35. https://doi.org/10.1007/s11095-018-2562-7.

Bolourchian, N., Talamkhani, Z., Nokhodchi, A., 2019. Preparation and physicochemical characterization of binary and ternary ground mixtures of carvedilol with PVP and SLS aimed to improve the drug dissolution. Pharm. Dev. Technol. 24, 1115–1124. https://doi.org/10.1080/10837450.2019.1641516.

Brokešová, J., Slámová, M., Zámostný, P., Kuentz, M., Koktan, J., Krejčík, L., Vraníková, B., Svačinová, P., Šklubalová, Z., 2022. Mechanistic study of dissolution

enhancement by interactive mixtures of chitosan with meloxicam as model. Eur. J. Pharm. Sci. 169, 106087 https://doi.org/10.1016/j.ejps.2021.106087.
Brunner, E., 1904. Reaktionsgeschwindigkeit in heterogenen systemen. Z. Phy. Chem. 47U, 56–102. https://doi.org/10.1515/zpch-1904-4705.
Butler, J.M., Dressman, J.B., 2010. The developability classification system: application of biopharmaceutics concepts to formulation development. J. Pharm. Sci. 99, 4940–4954. https://doi.org/10.1002/jps.22217.
Chingunpitak, J., Puttipipatkhachorn, S., Chavalitshewinkoon-Petmitr, P., Tozuka, Y., Moribe, K., Yamamoto, K., 2008. Formation, physical stability and in vitro antimalarial activity of dihydroartemisinin nanosuspensions obtained by co-grinding method. Drug Dev. Ind. Pharm. 34, 314–322. https://doi.org/10.1080/03639040701662388.
Fagerberg, J.H., Al-Tikriti, Y., Ragnarsson, G., Bergström, C.A.S., 2012. Ethanol effects on apparent solubility of poorly soluble drugs in simulated intestinal fluid. Mol. Pharm. 9, 1942–1952. https://doi.org/10.1021/mp2006467.
Grady, H., Elder, D., Webster, G.K., Mao, Y., Lin, Y., Flanagan, T., Mann, J., Blanchard, A., Cohen, M.J., Lin, J., Kesisoglou, F., Hermans, A., Abend, A., Zhang, L., Curran, D., 2018. Industry's view on using quality control, biorelevant, and clinically relevant dissolution tests for pharmaceutical development, registration, and commercialization. J. Pharm. Sci. 107, 34–41. https://doi.org/10.1016/j.xphs.2017.10.019.
Gu, F.G., Wang, Y., Meng, G.D.L., Han, H.B., Wu, C.Z., 2012. Investigation of a fenofibrate-hydroxypropyl-beta-cyclodextrin system prepared by a co-grinding method. Pharmazie 67, 143–146.
Ibraheem, B., Wagner, K.G., 2021. Influence of high pressure compaction on solubility and intrinsic dissolution of ibuprofen binary mixtures employing standard excipients. Int. J. Pharm. X. 3, 100075 https://doi.org/10.1016/j.ijpx.2021.100075.
Iemtsev, A., Zemánková, A., Hassouna, F., Mathers, A., Klajmon, M., Slámová, M., Malinová, L., Fulem, M., 2022. Ball milling and hot-melt extrusion of indomethacin–l-arginine–vinylpyrrolidone-vinyl acetate copolymer: solid-state properties and dissolution performance. Int. J. Pharm. 613, 121424 https://doi.org/10.1016/j.ijpharm.2021.121424.
Kah, M., Brown, C.D., 2008. LogD: lipophilicity for ionisable compounds. Chemosphere 72, 1401–1408. https://doi.org/10.1016/j.chemosphere.2008.04.074.
Kier, L.B., 1985. A shape index from molecular graphs. Quant. Structure-Act. Relationsh. 4, 109–116. https://doi.org/10.1002/qsar.19850040303.
Kim, J.H., 2019. Multicollinearity and misleading statistical results. Korean J. Anesthesiol. 72, 558–569. https://doi.org/10.4097/kja.19087.
Knieke, C., Sommer, M., Peukert, W., 2009. Identifying the apparent and true grinding limit. Powder. Technol. 195, 25–30. https://doi.org/10.1016/j.powtec.2009.05.007.
Kuentz, M., Bergström, C.A.S., 2021. Synergistic computational modeling approaches as team players in the game of solubility predictions. J. Pharm. Sci. 110, 22–34. https://doi.org/10.1016/j.xphs.2020.10.068.
Lim, A.W., Löbmann, K., Grohganz, H., Rades, T., Chieng, N., 2016. Investigation of physical properties and stability of indomethacin–cimetidine and naproxen–cimetidine co-amorphous systems prepared by quench cooling, coprecipitation and ball milling. J. Pharm. Pharmacol. 68, 36–45. https://doi.org/10.1111/jphp.12494.
Luciani, C.V., 2018. Impact of process parameters on the grinding limit in high-shear wet milling. Org. Process. Res. Dev. 22, 1328–1333. https://doi.org/10.1021/acs.oprd.8b00251.
Maggi, L., Bruni, G., Maietta, M., Canobbio, A., Cardini, A., Conte, U., 2013. I. Technological approaches to improve the dissolution behavior of nateglinide, a lipophilic insoluble drug: nanoparticles and co-mixing. Int. J. Pharm. 454, 562–567. https://doi.org/10.1016/j.ijpharm.2013.06.084.
Mahlin, D., Bergström, C.A.S., 2013. Early drug development predictions of glass-forming ability and physical stability of drugs. Eur. J. Pharm. Sci. 49, 323–332. https://doi.org/10.1016/j.ejps.2013.03.016.
Meiland, P., Larsen, B.S., Knopp, M.M., Tho, I., Rades, T., 2022. A new method to determine drug-polymer solubility through enthalpy of melting and mixing. Int. J. Pharm. 629, 122391 https://doi.org/10.1016/j.ijpharm.2022.122391.
Mura, P., Cirri, M., Faucci, M.T., Ginès-Dorado, J.M., Bettinetti, G.P., 2002. Investigation of the effects of grinding and co-grinding on physicochemical properties of glisentide. J. Pharm. Biomed. Anal. 30, 227–237. https://doi.org/10.1016/S0731-7085(02)00252-2.
Nernst, W., 1904. Theorie der Reaktionsgeschwindigkeit in heterogenen Systemen. Z. Phys. Chem. 47U, 52–55. https://doi.org/10.1515/zpch-1904-4704.
Niederquell, A., Kuentz, M., 2014. Biorelevant dissolution of poorly soluble weak acids studied by UV imaging reveals ranges of fractal-like kinetics. Int. J. Pharm. 463, 38–49. https://doi.org/10.1016/j.ijpharm.2013.12.049.
Ono, A., Kurihara, R., Terada, K., Sugano, K., 2023. Bioequivalence dissolution test criteria for formulation development of high solubility-low permeability drugs. Chem. Pharm. Bull. 71, c22–00685. https://doi.org/10.1248/cpb.c22-00685.
Patterson, J.E., James, M.B., Forster, A.H., Lancaster, R.W., Butler, J.M., Rades, T., 2007. Preparation of glass solutions of three poorly water soluble drugs by spray drying, melt extrusion and ball milling. Int. J. Pharm. 336, 22–34. https://doi.org/10.1016/j.ijpharm.2006.11.030.
Saharan, V., Kukkar, V., Kataria, M., Gera, M., Choudhury, P., 2010. Dissolution enhancement of drugs. part i: technologies and effect of carriers. Int. J. Health Res. 2 https://doi.org/10.4314/ijhr.v2i2.55401.
Slámová, M., Prausová, K., Epikaridisová, J., Brokešová, J., Kuentz, M., Patera, J., Zámostný, P., 2021. Effect of co-milling on dissolution rate of poorly soluble drugs. Int. J. Pharm. 597, 120312 https://doi.org/10.1016/j.ijpharm.2021.120312.
Varghese, S., Ghoroi, C., 2017. Improving the wetting and dissolution of ibuprofen using solventless co-milling. Int. J. Pharm. 533, 145–155. https://doi.org/10.1016/j.ijpharm.2017.09.062.
Vogt, M., Kunath, K., Dressman, J.B., 2008. Dissolution improvement of four poorly water soluble drugs by cogrinding with commonly used excipients. Eur. J. Pharm. Biopharm. 68, 330–337. https://doi.org/10.1016/j.ejpb.2007.05.009.
Yang, C., Xu, X., Wang, J., An, Z., 2012. Use of the co-grinding method to enhance the dissolution behavior of a poorly water-soluble drug: generation of solvent-free drug–polymer solid dispersions. Chem. Pharm. Bull. 60, 837–845. https://doi.org/10.1248/cpb.c12-00034.